

This is an Open Access document downloaded from ORCA, Cardiff University's institutional repository: <https://orca.cardiff.ac.uk/id/eprint/135011/>

This is the author's version of a work that was submitted to / accepted for publication.

Citation for final published version:

Pedziwiatr, Marek A., Kümmerer, Matthias, Wallis, Thomas S.A., Bethge, Matthias and Teufel, Christoph 2021. Meaning maps and saliency models based on deep convolutional neural networks are insensitive to image meaning when predicting human fixations. *Cognition* 206 , 104465. 10.1016/j.cognition.2020.104465

Publishers page: <http://dx.doi.org/10.1016/j.cognition.2020.104465>

Please note:

Changes made as a result of publishing processes such as copy-editing, formatting and page numbers may not be reflected in this version. For the definitive version of this publication, please refer to the published source. You are advised to consult the publisher's version if you wish to cite this paper.

This version is being made available in accordance with publisher policies. See <http://orca.cf.ac.uk/policies.html> for usage policies. Copyright and moral rights for publications made available in ORCA are retained by the copyright holders.



Meaning maps and saliency models based on deep convolutional neural networks are insensitive to image meaning when predicting human fixations

Marek A. Pedziwiatr^{1*}, Matthias Kümmeler², Thomas S.A. Wallis^{2, 3}, Matthias Bethge²,
Christoph Teufel¹

¹Cardiff University, Cardiff University Brain Research Imaging Centre (CUBRIC), School of Psychology
Cardiff, United Kingdom

²University of Tübingen, Center for Integrative Neuroscience, Tübingen, Germany

³Bernstein Center for Computational Neuroscience, Tübingen, Germany

*Corresponding author: marek.pedziwi@gmail.com

Abstract

Eye movements are vital for human vision, and it is therefore important to understand how observers decide where to look. Meaning maps (MMs), a technique to capture the distribution of semantic importance across an image, have recently been proposed to support the hypothesis that meaning rather than image features guide human gaze. MMs have the potential to be an important tool far beyond eye-movements research. Here, we examine central assumptions underlying MMs. First, we compared the performance of MMs in predicting fixations to saliency models, showing that DeepGaze II – a deep neural network trained to predict fixations based on high-level features rather than meaning – outperforms MMs. Second, we show that whereas human observers respond to changes in meaning induced by manipulating object-context relationships, MMs and DeepGaze II do not. Together, these findings challenge central assumptions underlying the use of MMs to measure the distribution of meaning in images.

Keywords: eye movements, natural scenes, saliency, deep neural networks, meaning maps

Introduction

31 Human eyes resolve fine detail only in a small, central part of the visual field, with resolution
32 dropping off rapidly in the periphery. To sample details, we move our eyes to orient the
33 high-resolution part of our visual system successively to different parts of a visual scene.
34 Information about these small scene parts is extracted during fixations – short periods in
35 which the eyes are relatively stable. Thus, due to the structure of our visual system, human
36 vision depends on eye movements. How the brain decides where to look in a visual scene is
37 therefore an important question. A long-standing hypothesis suggests that semantic content
38 of image regions is important in guiding eye movements. Recent work presented meaning
39 maps (MMs) as a tool to test this hypothesis (Henderson & Hayes, 2017, 2018). This
40 technique aims to index the spatial distribution of meaning across an image, which has
41 potential applications far beyond eye-movement research. Here, we assess and challenge
42 central assumptions of this novel tool.

43 A classic finding in eye-movement research shows that the specific task of an observer has
44 an influence on where they direct their eyes (Yarbus, 1967; Hayhoe & Ballard, 2005). But in
45 everyday life, we frequently move our eyes without any goal other than to explore the
46 environment. In the lab, this behavior is examined in free-viewing paradigms, during which
47 eye movements are recorded while images are viewed without an explicit task (Koehler,
48 Guo, Zhang, & Eckstein, 2014, but see Tatler, Hayhoe, Land, & Ballard, 2011). To explain
49 what guides eye movements during free viewing, two opposing accounts have been put
50 forward.

51 According to the first account, eye movements are guided primarily by image characteristics
52 (Borji, Sihite, & Itti, 2013; Itti & Koch, 2001; Parkhurst, Law, & Niebur, 2002). Potential
53 support for this view comes from saliency models: algorithms, which exclusively use visual
54 features of an image to predict human fixations. Although early models, which used only
55 simple features such as local intensity or colors (Itti & Koch, 2000), are now deemed only
56 moderately successful (Bylinskii et al., 2014), more recent saliency models achieve a
57 remarkably high performance (Kümmerer, Wallis, Gatys, & Bethge, 2017). These models
58 harness deep convolutional neural networks – biologically inspired machine learning
59 algorithms, that somewhat resemble the human visual system (Kietzmann, McClure, &
60 Kriegeskorte, 2019). However, even such models rely solely on visual features, albeit high-
61 level ones.

62 In contrast to the idea underlying saliency models, several authors have argued that during
63 free viewing, eye movements are mainly guided by the semantic content of the visual scene
64 (Henderson, Malcolm, & Schandl, 2009; Nyström & Holmqvist, 2008; Onat, Açik, Schumann,
65 & König, 2014; Rider, Coutrot, Pellicano, Dakin, & Mareschal, 2018; Stoll, Thrun, Nuthmann,
66 & Einhäuser, 2015). This perspective differs fundamentally from the saliency-based
67 approach. Attributing meaning to certain parts of the scene is impossible without prior
68 knowledge of the world, i.e., a factor that is independent of the visual input (Hegde &
69 Kersten, 2010; Teufel, Dakin, & Fletcher, 2018). Consequently, the notion that semantic
70 content guides eye-movements is inconsistent with the idea that the allocation of fixations
71 is dependent solely on the distribution of image features. Given that meaning is not image-
72 computable, the notion that semantic content guides eye-movements is inconsistent with
73 the idea that the eye-movements are dependent solely on the distribution of image
74 features.

75 A string of recent studies has claimed to provide support for the role of meaning in driving
76 eye movements (Hayes & Henderson, 2019; Henderson & Hayes, 2017, 2018; Henderson,
77 Hayes, Rehrig, & Ferreira, 2018; Peacock, Hayes, & Henderson, 2018). These studies
78 (reviewed in Henderson, Hayes, Peacock, & Rehrig, 2019) are based on a novel technique
79 called meaning maps (MMs). A MM for a given image is created by breaking it down into
80 small isolated patches, which are rated for their meaningfulness independently from the
81 rest of the visual scene. These ratings are pooled together into a smooth map, which is
82 supposed to capture the distribution of meaning across the image. Compared to outputs
83 from a simple saliency model (GBVS, Harel et al., 2006), MMs were more predictive of
84 human fixations. On that basis it has been claimed that meaning guides human fixations in
85 natural scene viewing (Henderson & Hayes, 2017, 2018). Here, we examined central
86 predictions of this claim.

87 First, if MMs measure meaning and if meaning guides human eye-movements, MMs should
88 be better in predicting locations of fixations than saliency models because these models rely
89 solely on image features. Therefore, we compared MMs to a range of classic and state-of-
90 the-art models. We replicate the finding that MMs perform better than some of the most
91 basic saliency models. Contrary to the prediction, however, DeepGaze II (DGII; Kümmerer,

92 Wallis, & Bethge, 2016; Kümmerer et al., 2017), a model based on a deep convolutional
93 neural network, outperforms MMs.

94 A second prediction is that if MMs are sensitive to meaning and if meaning guides human
95 gaze, differences in eye movements that result from changes in meaning should be reflected
96 in equivalent differences in MMs. We probed this prediction experimentally using a well-
97 established effect: the same object, when presented in an atypical context (e.g., a shoe on a
98 bathroom sink) attracts more fixations than when presented in a typical context because of
99 the change in the semantic object-context relationship (Henderson, Weeks, & Hollingworth,
100 1999; Öhlschläger & Vö, 2017). Replicating previous studies, image regions attracted more
101 fixations when they contained context-inconsistent compared to context-consistent objects.
102 Crucially, however, MMs of the modified scenes did not attribute more 'meaning' to these
103 regions. DGII also failed to adjust its predictions accordingly.

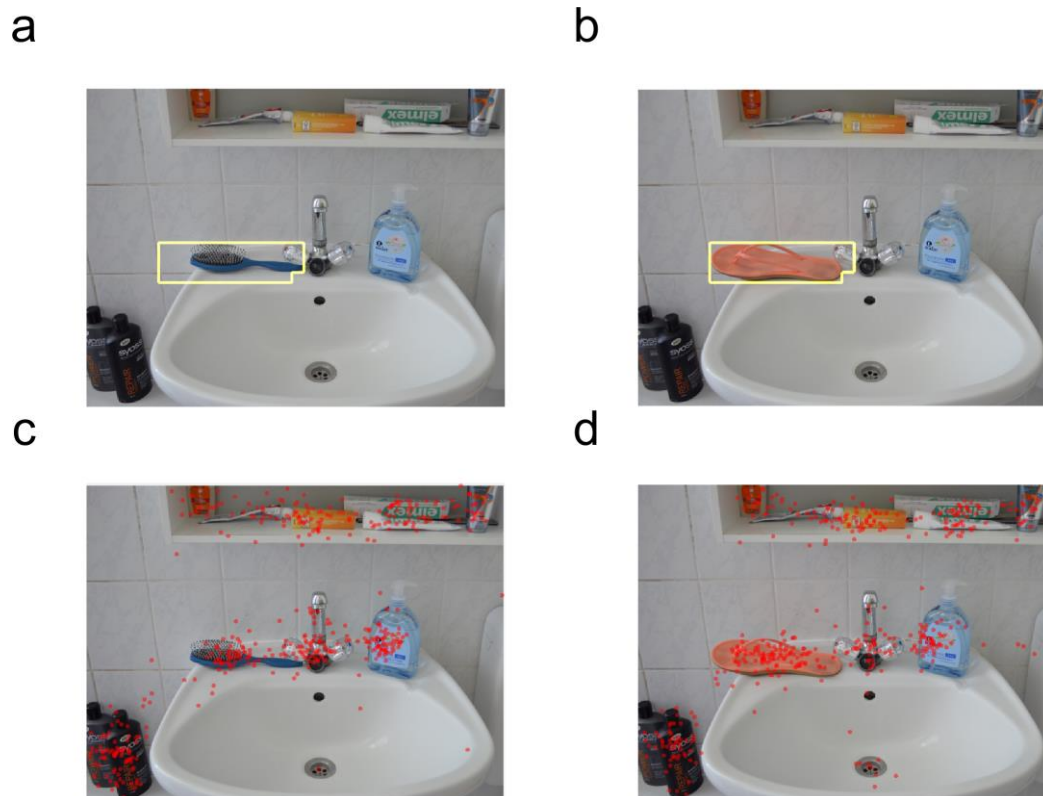
104 Together, these findings suggest that semantic information contained in visual scenes is
105 critical for the control of eye movements. However, this information is captured neither by
106 MMs nor DGII. We suggest that similar to saliency models, MMs index the distribution of
107 visual features rather than meaning.

108

109

Method

110 We conducted a single experiment in which human observers free-viewed natural scenes
111 while their eye-movements were being recorded. The obtained data was analyzed in two
112 complimentary ways. First, we compared how well MMs and different saliency models
113 predict locations of human fixations in natural scenes. Subsequently, we assessed the
114 sensitivity of MMs and the best-performing saliency model to manipulations of scene
115 meaning. The data, the code to create MMs, and all openly available resources used in the
116 study can be accessed via the links provided in the Supplement.



117

118 Fig. 1. Illustration of sample stimuli in (a) the Consistent and (b) the Inconsistent condition
119 with the Critical Region outlined in yellow and (c, d) human fixations recorded in both
120 conditions. In this example, a hair brush on a bathroom sink (a) – an object consistent with
121 the scene context – has been exchanged for a shoe (b) to introduce semantic inconsistency.

122

123 **Stimuli.** We used images from two conditions of the SCEGRAM database (Öhlschläger & Vö,
124 2017): the Consistent and the Semantically Inconsistent conditions (called ‘Inconsistent’
125 here). In the Consistent condition (used in both analyses), scenes contain only objects that
126 are typical for a given context. In the Inconsistent condition (used only in the second
127 analysis), one of the objects is contextually inconsistent. For example, a hairbrush in the
128 context of a bathroom sink from the Consistent condition is replaced with a flip-flop in the
129 Inconsistent condition (see Figs. 1a and 1b). Such changes in object-context relationship
130 alter the meaning attached to the manipulated object. For every scene, we indexed the
131 location of the consistent and inconsistent objects with the superimposed bounding boxes
132 for both objects (see Figs. 1a and 1b). We refer to this location as the Critical Region,
133 because it is the only part of the image that changes between Consistent and Inconsistent
134 conditions. We used 36 selected scenes in both conditions (72 photographs in total, listed in

135 the Supplement together with the selection criteria). We also replicated the main finding of
136 the first analysis in an additional set of 30, very different, images (reported in the
137 Supplement).

138

139 **Procedure.** The procedure consisted of 3 blocks, interleaved with breaks. Each participant
140 viewed all images from both conditions (Consistent and Inconsistent) and was instructed to
141 'look carefully' at each of them. Experimental blocks began with an eye tracker
142 calibration/validation. Within each block, observers free-viewed a series of 24 photographs
143 from both SCEGRAM conditions, each for 7 seconds. After image offset, observers were
144 required to press a button to view the next image. Then, a fixation point appeared centrally
145 on a screen and once observers fixate on it (as determined online by their eye-trace), the
146 actual image was displayed. Before starting the experiment, observers viewed a sample
147 image in an identical regime to familiarize themselves with the procedure. Each stimulus
148 was shown once and the order of presentation was fully randomized. The stimuli were
149 presented against a uniform grey background and had a width of 688 pixels and a height of
150 524 pixels, which subtended approximately 19.7 and 15 degrees of visual angle,
151 respectively. Our choice of task (free viewing) and stimulus parameters for size and
152 presentation time were adopted from the original study developing the SCEGRAM stimuli
153 (Öhlschläger & Vö, 2017). These design characteristics fall within the typical range used in
154 this literature (e.g. Wilming et al., 2017).

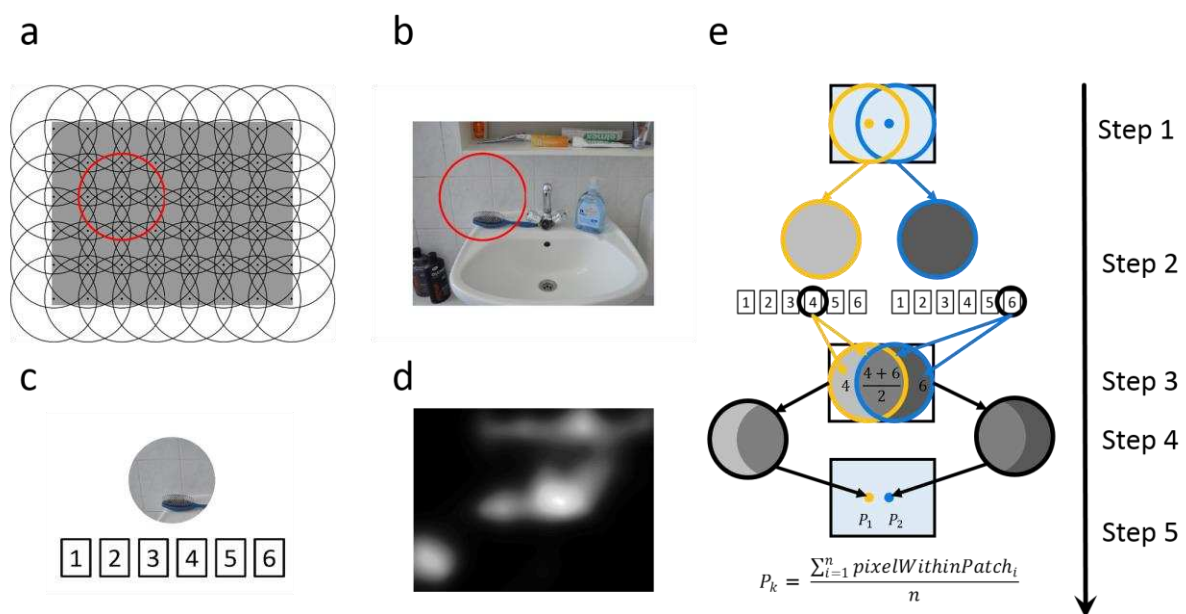
155

156 **Observers.** 20 volunteers (3 male; mean age 19.4) recruited from the Cardiff University
157 undergraduate population took part in the study. All reported normal or corrected-to-
158 normal vision, provided written consent, and received course credits in return for
159 participation. The study was approved by the Cardiff University School of Psychology
160 Research Ethics Committee. The primary units of interest in our analyses were the
161 distributions of fixations over images. The number of observers we recruited guarantees
162 that including more observers would not change these distributions significantly
163 (demonstrated in the Supplement).

164

165 **Apparatus.** The study was conducted in a dimly lit room. SCEGRAM images from both
 166 conditions were presented on an LCD monitor (Iiyama ProLite B2280HS, resolution 1920 by
 167 1080 pixels, 21 inches diagonal). Chin and forehead rests were used to ensure that
 168 observers maintained the constant distance of 49 cm from the screen. Their eye movements
 169 were recorded with the frequency of 500 Hz using an EyeLink 1000+ eye tracker placed on a
 170 tower mount. The experiment was controlled by custom-written Matlab (R2017a version)
 171 scripts using Psychophysics Toolbox Version 3 (Kleiner, Brainard, & Pelli, 2007).

172



173

174 Fig. 2. Illustration of the stimuli and procedure used for creating meaning maps. (a) Grids of
 175 equally spaced circles were used to cut images into fine and coarse patches (only the latter
 176 are illustrated here). The red circle indicates a sample patch in the grid. (b) Here, the sample
 177 patch is highlighted in one of the scenes from the Consistent condition. (c) Patches were
 178 presented in isolation and rated for their meaningfulness by three independent observers
 179 on a scale from 1 to 6. The panel has illustrative purpose only – the scale presented to
 180 observers included additional labels (ranging from ‘Very Low’ to ‘Very High’). (d) Illustration
 181 of a meaning map with greyscale values indicating ‘meaningfulness’. (e) Simplifying
 182 illustration of how meaning maps are generated from ratings. For simplicity sake, only two
 183 patches are shown (step 1). Each patch is rated in isolation (step 2; here only one rating per
 184 patch is shown). All pixels within an image area are then assigned average rating values,

185 taking into account all ratings for patches that overlap with this area (step 3). For the area of
186 the original patch (step 4), all pixels are then averaged and the resulting value is assigned to
187 the center of the patch (step 5). Finally, the patch centers were used as interpolation nodes
188 for thin-plate spline interpolation producing a smooth distribution of values over the image
189 (not illustrated). This procedure was conducted separately for the fine and coarse grid, and
190 the meaning map for a given image was created by averaging the two outcomes and
191 normalizing the result to a range between 0 and 1.

192

193 **Creating MMs.** To create MMs for our stimuli, we followed the procedure described by
194 Henderson & Hayes (2017, 2018; for details see Fig. 2). Each image was segmented into
195 partially overlapping patches of two sizes: fine patches had a diameter of 107 pixels (3
196 degrees of the visual angle, or 16 % of the image width), coarse patches of 247 pixels (7
197 degrees or 36% of the image width) (Fig. 2a and b). Their centers were 58 pixels (fine) and
198 97 pixels (coarse) apart from each other.

199 Next, we collected meaningfulness ratings from human subjects for all patches. Each patch
200 was presented in isolation and rated for its meaningfulness on a 6 point Likert scale (Fig. 2).
201 As in Henderson and Hayes (2017), we used a Qualtrics survey completed by naive
202 observers recruited via the crowdsourcing platform Amazon Mechanical Turk (see
203 Supplement for eligibility criteria). Each participant provided ratings for 305 or 303 patches
204 of both sizes (selected randomly from all images), on average spent approximately 14 min
205 on the task, and received 2.18 USD as remuneration. In total, 69 individuals were used as
206 raters, with three individuals rating each individual patch. The collected ratings were then
207 used to create MMs (see Fig. 2).

208 When creating MMs for images from both conditions, we exploited the fact that
209 photographs from the Consistent and Inconsistent conditions differ only in the Critical
210 Region (the part of the image containing the manipulated object) while the remaining parts
211 overlap. We collected meaningfulness ratings for the patches belonging to overlapping
212 areas only once, and the separate sets of ratings for Consistent and Inconsistent condition
213 were collected only for those patches that contained at least one pixel belonging to the
214 Critical Region. In total, the number of patches rated in the study amounted to 7013: 4840

215 fine patches (of which 520 belonged to the images from the Inconsistent condition) and
216 2173 coarse patches (445 Inconsistent).

217

218 **Saliency models.** In the first analysis, we compared predictive performance of MMs to four
219 saliency models of different complexity. The first two models – GBVS (Harel et al., 2006) and
220 AWS (Garcia-Diaz, Fdez-Vidal, Pardo, & Dosil, 2012) – rely on simple visual features, such as
221 local colors and edge orientations, and share the assumption that fixations land on image
222 regions distinct from their surroundings in terms of values of these features. By contrast to
223 GBVS, AWS includes a statistical whitening procedure to improve performance. Both these
224 models were previously used to estimate the influence of image features relative to
225 cognitive factors on the deployment of fixations: GBVS in the previous studies with MMs,
226 AWS elsewhere (Stoll et al., 2015).

227 Two other models that we compared to MMs – ICF and DeepGaze II (DGII) – were designed
228 in a data-driven manner (Kümmerer et al., 2017). Both have the same architecture,
229 consisting of a fixed network that extracts sets of features from images and a readout
230 network that is trained on human fixations to combine the features in a way to maximize
231 the models' predictive power. While the fixed network of ICF extracts only simple visual
232 features (local intensity and contrast), DGII is tuned to features extracted by a deep
233 convolutional neural network pre-trained for object recognition (VGG-19; Simonyan &
234 Zisserman, 2014). The key characteristic of these models that distinguishes them from
235 models such as GBVS and AWS is that they have been trained on human fixations.
236 Specifically, during the training phase, the read-out network receives its respective features
237 as an input, generates a prediction about where human observers will look in the image,
238 and gradually adjusts its parameters based on feedback comparing its prediction to human
239 fixation data to maximise the predictive power of each model. Importantly, the readout
240 network has the same architecture and number of trainable parameters for both DGII and
241 ICF. The only difference between the models is the input features, both of which are not
242 trained on human fixation data.

243 All saliency models output smooth maps that predict the probability of image regions to be
244 fixated. Human observers have the tendency to look at the center of images (Tatler, 2007),

245 and therefore this probability is usually higher in the central region of the image. This
246 ‘center bias’ has important consequences for the evaluation of saliency models. Their
247 performance differs depending on whether they are evaluated using a metric expecting
248 some form of this bias or not (Kümmerer, Wallis, & Bethge, 2018). Here, for the sake of
249 simplicity, we do not incorporate center bias in the models or in the MMs (unlike the
250 original authors) and use an appropriate metric for this situation (see Performance metrics
251 section). Importantly, analyses addressing the issue of center bias in a more extensive way
252 (reported in the Supplement) provide only further support for our conclusions.

253

254 **Data pre-processing.** Fixation locations from the eye tracker recordings were extracted
255 using the algorithm provided by the device manufacturer operating with the default
256 parameter values. Thereby, we obtained a discrete distribution of fixations on each image
257 (see Fig. 1c and 1d). Then, in line with the previous MMs studies, we smoothed these
258 discrete distributions with a Gaussian filter with a cutoff frequency of -6 dB, using the
259 function provided by Bylinskii and colleagues (2014).

260 Next, smooth distributions from fixations, models, and MMs were separately normalized to
261 a range from 0 to 1 for each image. Finally, for each scene, histograms of all distributions
262 from both conditions were matched to histograms of smoothed fixations from Consistent
263 condition using the Matlab `imhistmatch` function, as in the original MMs studies. Histogram
264 matching makes distributions directly comparable as it ensures that they differ only with
265 respect to their shape, and not their total mass.

266

267 **Performance metrics.** To compare the ability of MMs and models to predict locations of
268 human fixations in Experiment 1, we use two well-established metrics (Bylinskii, Judd, Oliva,
269 Torralba, & Durand, 2016): Correlation and Shuffled Area Under ROC curve (sAUC; Zhang,
270 Marks, Tong, Shan, & Cottrell, 2007) with the implementations provided by Bylinskii and
271 colleagues (2014).

272 Correlation, used in the previous studies on MMs, is calculated as Pearson's linear
273 correlation coefficient between a smoothed distribution of observers' fixations over the

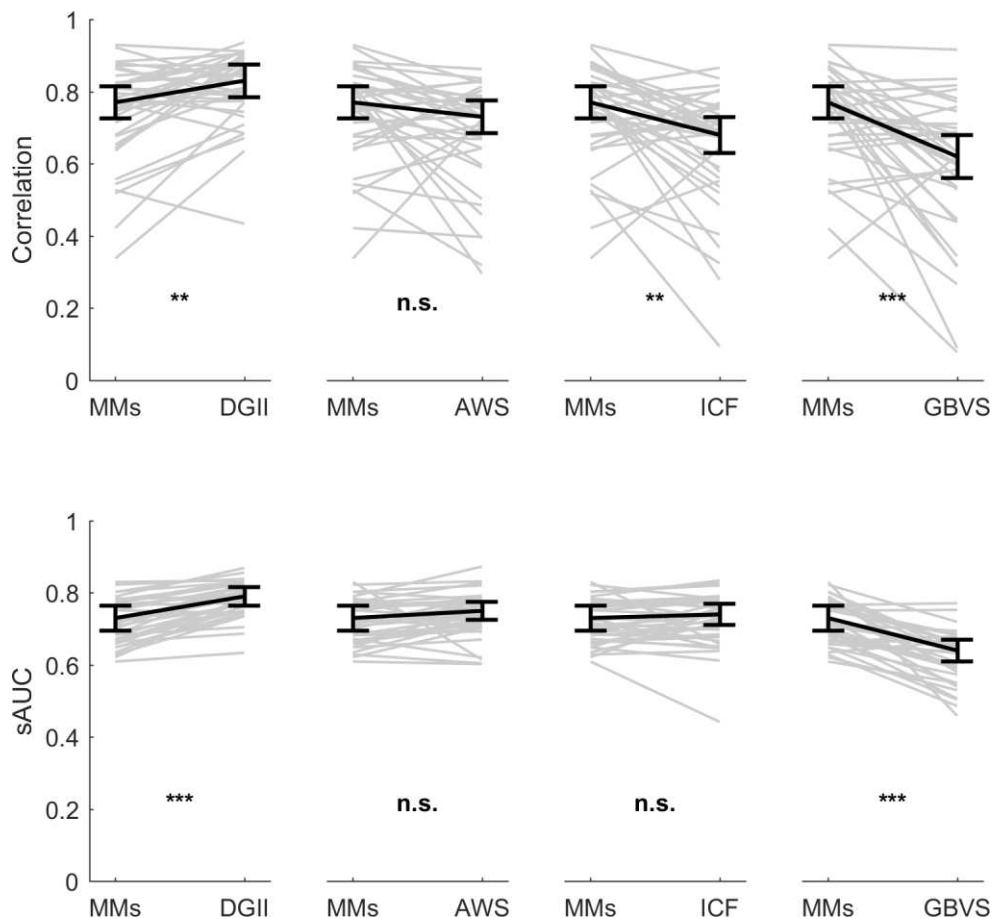
274 image and predictions of a saliency model or MMs. We additionally used sAUC (Zhang et al.,
275 2008), which, unlike Correlation, guarantees that the measured differences in performance
276 between models are driven by their sensitivity to factors guiding fixations, and not by the
277 degree to which they include human center bias in their predictions, even implicitly
278 (Kümmerer, Wallis, & Bethge, 2015; Kümmerer et al., 2018).

279

280 **Comparing meaning maps and saliency models – results**

281 In the first analysis, we compared performance of four saliency models to MMs in predicting
282 human fixations in the Consistent condition, i.e., when viewing typical scenes with no
283 obvious object-context inconsistencies (Tab. 1, Fig. 3). If human gaze is guided by meaning,
284 and if MMs provide an index for the distribution of meaning, we would expect MMs to
285 outperform all saliency models because these models are based solely on image features.
286 Please note that for the sake of this comparison, we aggregated fixations from all observers
287 for each image and analyzed the data on a per-image basis, similarly to the original MMs
288 studies.

289



290

291

292 Fig. 3. Performance of MMs and saliency models in predicting human fixations according to
 293 (a) Correlation and (b) sAUC metrics. Note that according to both metrics DGII predicted
 294 human fixations better than MMs. Asterisks indicate p-values from statistical tests
 295 comparing MMs to different models (reported in Table 1.): * indicates $p \leq .05$, ** $p \leq .01$,
 296 *** $\leq .001$ and 'n.s.' indicates the lack of statistical significance. Grey lines connect values
 297 obtained for individual images. Black vertical bars indicate 95% confidence intervals for the
 298 medians.

299

300 **Predictive power.** Correlation and sAUC values obtained for MMs and for each of the
 301 models were compared using Bonferroni-corrected paired Wilcoxon tests (Fig. 3; Tab. 1).
 302 We used non-parametric tests because for some of the distributions the assumptions of
 303 normality was not met. For the same reason we chose a median as a measure of centrality
 304 (we calculate confidence intervals for median using a bootstrapping method – see details in

305 the Supplement). Additionally, we calculated JZS Bayes Factor (Rouder, Speckman, Sun,
 306 Morey, & Iverson, 2009) to quantify the evidence for (or against) the differences between
 307 models and MMs (Tab. 1). While deviations from normality can be problematic for Bayes
 308 factor analyses, they are most likely not an issue in the current situation: the Bayes factors
 309 for the key finding are large and the deviations from normality are small.

310 As shown in Tab. 1 and on Fig. 3, according to both measures, MMs outperformed GBVS in
 311 predicting human fixations, thereby replicating the results of Henderson and Hayes (2017,
 312 2018) using new images and new participants. Contrary to expectations, however, both
 313 metrics indicated that DGII predicted fixations better than MMs. Furthermore, performance
 314 of AWS and MMs did not differ significantly irrespective of the metrics. Finally, MMs
 315 outperformed ICF according to Correlation, but not sAUC. In fact, for the latter metric, JZS-
 316 Bayes Factor indicated support for the null hypothesis.

317

318 Table 1. Comparison of Predictive Power of Saliency Models and MMs Using Correlation and
 319 sAUC.

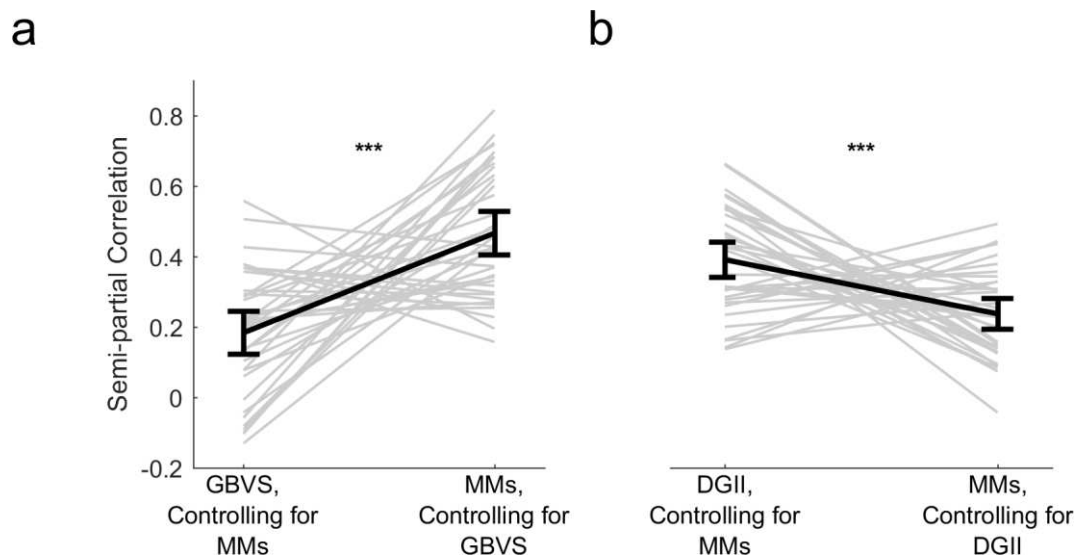
Model	Median of prediction values with 95% confidence intervals	Median of differences from MMs with 95% confidence intervals	W statistic	p-value (Bonferroni-corrected)	JZS Bayes Factor
Correlation					
DGII	0.83 [0.78, 0.87]	0.07 [0.03, 0.11]	526	0.00738	32.26
MMs	0.77 [0.72, 0.81]	–	–	–	–
AWS	0.73 [0.67, 0.76]	-0.06 [-0.12, -0.01]	192	0.10412	1.48
ICF	0.68 [0.61, 0.71]	-0.12 [-0.18, -0.06]	144	0.00936	16.90
GBVS	0.62 [0.56, 0.68]	-0.11[-0.26, -0.05]	94	< .001	396.96
sAUC					
DGII	0.79 [0.77, 0.82]	0.06 [0.05, 0.08]	662	< .001	> 1000
MMs	0.73 [0.69, 0.76]	–	–	–	–
AWS	0.75 [0.72, 0.77]	0.02 [0.01, 0.04]	490	0.0507	0.60
ICF	0.74 [0.70, 0.76]	0.01 [-0.01, 0.02]	383	1.00	0.19
GBVS	0.64 [0.60, 0.66]	-0.10 [-0.12, -0.08]	13	< .001	> 1000

320

321 **Semi-partial correlations.** Because predictions of models and MMs overlap, we quantified
 322 their distinct predictive power using semi-partial correlations. We conducted these analyses
 323 for GBVS (used in the original MMs studies) and DGII (the only model which markedly
 324 outperformed MMs).

325 For each scene from the Consistent condition, we calculated two semi-partial correlations
 326 with the distribution from smoothed fixations: one for MMs while controlling for GBVS, and
 327 one for GBVS while controlling for MMs (see Fig. 4). Consistent with findings by Henderson
 328 and Hayes (2018), MMs explain more unique variance than GBVS (Fig. 6a), as indicated by
 329 the significantly higher coefficients in the former than the latter case (mean difference 0.28,
 330 95% confidence interval (CI) [0.17, 0.39]; paired t-test, $t(35) = 5.22$, $p < .001$). Interestingly,
 331 the identical analysis with DGII revealed that DGII explained significantly more unique
 332 variance than MMs (mean difference 0.15, 95% CI [0.07, 0.24]; $t(35) = 3.60$, $p < .001$, see
 333 also Fig. 4b).

334



335

336 Fig. 4. Comparison of semi-partial correlations with smoothed human fixations for (a) MMs
 337 and GBVS and for (b) MMs and DGII. The obtained coefficients were significantly higher
 338 when assessing MMs while controlling for GBVS compared to when assessing GBVS when
 339 controlling for MMs. The opposite was true for the analyses with DGII. All figure
 340 characteristics are as in Fig. 3. except that means instead of medians are presented.

341

342 **Internal replication.** To demonstrate the generalizability of our conclusions beyond
343 SCEGRAM images, we replicated the main results with a different stimulus set (see the
344 Supplement).

345

346 **Comparing meaning maps and saliency models – discussion**

347 If human gaze is guided by meaning, and if MMs index the distribution of meaning across an
348 image, MMs should outperform saliency models that are exclusively based on image
349 features. Our first analysis showed that this prediction does not hold. In fact, DGII generated
350 better predictions and explained more unique variance than MMs. Therefore, at least one of
351 the two premises of our prediction is wrong: either human eye-movements are not sensitive
352 to meaning or MM do not index meaning. The second analysis allowed us to distinguish
353 between these alternatives.

354

355 **Analyzing the effects of semantic inconsistencies within scenes – method**

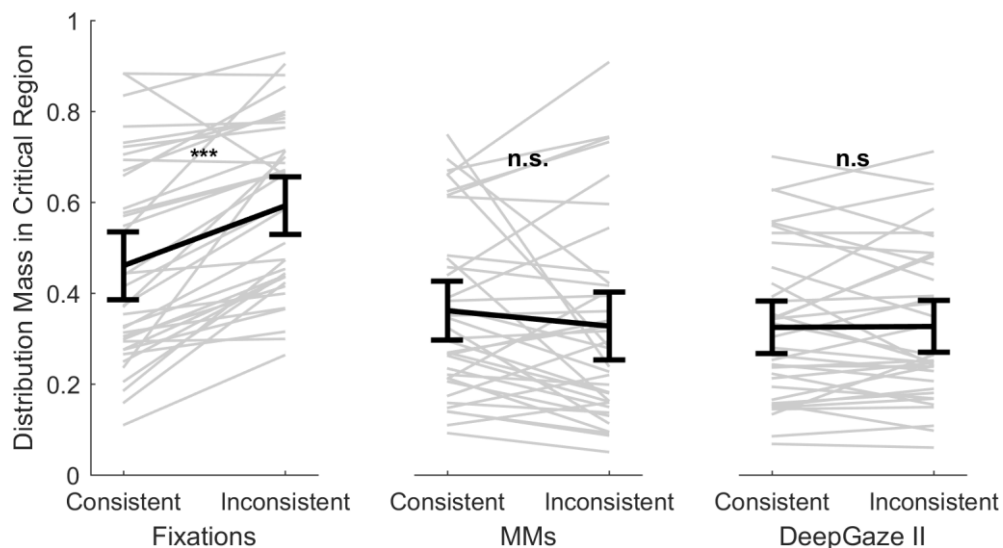
356 In the second analysis, we assessed how human observers, DGII, and MMs respond to
357 experimental changes in meaning induced by altered object-context relationships. We used
358 eye-movement data from both the Consistent and the Inconsistent condition. These
359 conditions differed solely in the Critical Region, an area that either contained an object that
360 was either consistent with the scene context or induce semantic conflict. For each scene, we
361 calculated the mass of the distributions of human gaze, DGII, and MMs falling into the
362 Critical Region, respectively, and divided it by the Region's area for normalization. Our
363 primary interest was the comparison between conditions: to the extent to which humans,
364 DGII, and MMs are sensitive to meaning, they should fixate more (humans) or predict more
365 fixations (DGII and MMs) on the Critical Region in the Inconsistent than the Consistent
366 condition.

367

368 **Analyzing the effects of semantic inconsistencies within scenes – results**

369 Our comparison indicated that, as predicted, observers fixated more on inconsistent than
 370 consistent objects (Fig. 5a). By contrast, behavior of both MMs and DGII did not change
 371 across conditions (Fig. 5b and c). These impressions were confirmed by a 2x3 ANOVA, with
 372 condition (Consistent vs. Inconsistent) as a within-subjects factor and the distribution source
 373 (human fixations vs. MMs vs. DGII) as a between-subjects factor. We found a statistically
 374 significant main effect of distribution source, $F(2, 105) = 13.09, p < .001, \omega^2 = 0.16$ and
 375 condition, $F(1, 105) = 7.41, p = 0.0076, \omega^2 = 0.005$. These main effects were qualified by a
 376 significant interaction, $F(2, 105) = 16.90, p < .001, \omega^2 = 0.026$. Tukey post-hoc tests showed
 377 that human observers looked more at the Critical Regions in the Inconsistent, than the
 378 Consistent condition, $t(105) = -6.22, p < .001$. In contrast, no significant differences between
 379 conditions were found for DGII, $t(105) = -0.09, p = 1.0$, and MMs, $t(105) = 1.60, p = 0.6028$.
 380 Comparisons within conditions indicated that human fixations differed from MMs in the
 381 Inconsistent condition, $t(129.91) = 5.78, p < .001$, but not the Consistent condition, $t(129.91)$
 382 $= 2.16, p = 0.2662$. A significant difference between DGII and human fixations was detected
 383 in both Consistent, $t(129.91) = -2.96, p = 0.0420$, and Inconsistent conditions, $t(129.91) = -$
 384 $5.79, p < .001$.

385



386

387 Fig. 5. Normalized distribution mass falling within Critical Regions in both conditions for (a)
 388 smoothed human fixations, (b) MMs, and (c) DGII. All figure characteristics are as in Fig. 3.

389

390 Additionally, conditions differed regarding the number of fixations per image, $t(35) = 5.67$ p
391 $< .001$. On average, there were 6% fewer fixations in the Inconsistent condition. This
392 excludes the possibility that higher number of fixations in this condition might drive the
393 observed increase in the distribution mass falling within the Critical Regions.

394 Any systematic differences in object size between Consistent and Inconsistent conditions
395 also could affect our results because larger objects may attract more fixations solely
396 because they occupy a larger image area. However, this factor was minimized by showing
397 each object in a consistent and an inconsistent context. Yet, the same object might be
398 shown in a slightly different position in the two conditions and might therefore occupy
399 slightly different amounts of the image. This was, however, not the case: the JZS Bayes
400 Factor of 4.26 indicated that the two conditions did not differ in the size of the bounding
401 boxes of each manipulated object (objects in the Inconsistent condition were on average
402 1562.28 pixels larger; 95% confidence interval: [-2582.74, 5707.29]).

403 Next, please note that we employed a within-subject design, which might have led to carry-
404 over effects: observer viewing a given scene in the Inconsistent condition first could be
405 biased to look at the Critical Region in the Consistent condition when they viewed the same
406 scene for a second time. Note that even if this unwanted phenomenon occurred despite a
407 randomised order of stimuli presentation, it could only decrease the magnitude of the
408 effects of interest.

409 Finally, it is possible that our observers implicitly engaged in a task. Specifically, once the
410 observers realized that the stimuli contain object-context inconsistencies, they might have
411 started actively searching for them. Engaging in this semantic oddball-search task would
412 result in very different spatial distributions of fixations compared to the ones that would be
413 obtained during free-viewing. This prediction was not supported by our findings: we
414 replicated our main experiment in a different set of observers with images that did not
415 contain semantic inconsistencies, and found that DGII still predicted fixation locations better
416 than MMs. This separate data set, therefore, suggests that observers did not engage in an
417 oddball search task and that the superiority of DGII is not specific to SCEGRAM images only
418 (details to be found in the Supplement).

419 To summarize, semantic changes induced by altering object-context relationships elicited
420 changes in distributions of human fixations, but neither MMs nor DGII could predict them.
421 These results suggest that both models might be sensitive to image features, which are
422 frequently correlated with image meaning, rather than to meaning itself.

423

424

Discussion

425 A long-standing debate in visual perception concerns the extent to which visual features vs.
426 semantic content guide human eye-movements in free viewing of natural scenes. To
427 distinguish these hypotheses, indexing the distributions both of features and meaning
428 across an image is critical. While image-based saliency models have been used to index
429 features for two decades, measuring semantic importance has been difficult until meaning
430 maps (MMs) have recently been proposed. Here, we assessed the extent to which MMs
431 indeed capture the distribution of meaning across an image. First, we demonstrate that
432 despite the purported importance of meaning as measured by MMs for gaze control, MMs
433 are not better predictors of locations of human fixations than at least some saliency models,
434 which are based solely on image features. In fact, DeepGaze II (DGII), a model using deep
435 neural network features, outperformed MMs. Second, we assessed the sensitivity of human
436 eye-movements, MMs, and DGII to changes in image meaning induced by violations of
437 typical object-context relationships. Observers fixated more often on regions containing
438 objects inconsistent with scene context (thus replicating previous findings) but these regions
439 were not indexed as more meaningful by MMs, or as more salient by DGII. Together, these
440 findings challenge central assumptions of MMs, suggesting that they are insensitive to the
441 semantic information contained in the stimulus.

442 The good performance of DGII in predicting human gaze might be attributable to the high-
443 level features it extracts from images. Three other models, which use low-level features,
444 failed to decisively outperform MMs. However, unlike two of them (GBVS and AWS), DGII is
445 trained with data on human fixations to optimize performance (Kümmerer et al., 2016,
446 2017). Yet, training alone cannot explain the difference in performance. The third low-level
447 feature model (ICF) is trained in the same way (Kümmerer et al., 2017) but still achieves a
448 lower performance than DGII. These findings suggest that feature type is indeed critical for a

449 model's performance. Importantly, however, while DGII uses high-level features transferred
450 from a deep neural network trained on object recognition (Simonyan & Zisserman, 2014),
451 this is not equivalent to indexing meaning. Rather, the good performance of DGII is likely
452 due to meaning supervening on, or correlating with, some of the features indexed by this
453 model.

454 Correlation between visual features and meaning as the source of good performance in
455 saliency models has already been considered by the authors of MMs (Henderson & Hayes,
456 2017). Our findings suggest that MMs might share this characteristic with saliency models.
457 Specifically, the ratings used to construct MMs might be based on visual properties in such a
458 way that highly structured patches that contain high-level features receive high ratings.
459 These features often correlate with meaning, but in and of themselves do not amount to
460 meaning. According to this interpretation, both DGII and MMs index high-level features.
461 Their success in predicting human behavior derives from the typically strong correlation
462 between high-level features and meaning, with a higher correlation for the features
463 extracted by DGII than MMs.

464 An alternative interpretation of the finding that DGII outperforms MMs is that image
465 features rather than meaning guide human fixations. However, this interpretation is
466 inconsistent with our second analysis. Here, observers clearly exhibited sensitivity to
467 meaning, as indicated by changes in gaze-patterns elicited by introducing semantic
468 inconsistencies into the images. This experimental manipulation targets a type of meaning
469 that is based on how objects relate to the broader context in which they occur. While
470 specific, it is precisely this kind of meaning that is of high theoretical importance in eye-
471 movement research (Henderson, 2017; 429 Henderson et al., 2009). Natural scenes are
472 composed of multiple objects, and the physical and semantic relationships between these
473 objects as well as their relationship to the scene gist, determine the meaning of a scene
474 (Kaiser et al., 2019; Malcolm et al., 2016; Vö et al., 2019). Thus, the fact that MMs are not
475 sensitive to the meaning derived from object-context relationships seriously limits their
476 usefulness.

477 It is, however, possible that – as has been already suggested (Henderson et al., 2018) – MMs
478 capture some form of 'local' meaning that is important for oculomotor control. Evaluating

479 our results in this respect is complicated by the correlation between features and meaning
480 (Elazary & Itti, 2008), which we already alluded to above. Yet, at the very least, the fact that
481 MMs do not consistently outperform even simple saliency models such as AWS that by
482 design rely on low-level image features warrants caution. This finding indicates that either
483 the purported kind of meaning indexed by MMs is not of primary importance for guidance
484 of eye-movements, or that it is almost perfectly correlated with the features indexed by
485 models such as AWS. A similar issue relates to DGII: while our study shows that this model
486 does not index meaning derived from object-context relationships, one might argue that it
487 acquires sensitivity to some (local) form of meaning by virtue of being trained on human
488 data. Specifically, if eye-movements are guided by the semantic content of images, then
489 training on eye-movement data might lead to developing ‘meaning-sensitivity’ in the model.
490 While this scenario cannot be ruled out for the same reasons as in the case of MMs, recall
491 that the ICF model – which uses simpler features than DGII – is also trained on human data
492 but fails to reach the high performance of DGII. Therefore, if the high performance of DGII is
493 based on some form of ‘local’ meaning, then it is not training per se that leads to the
494 development of this meaning but an interaction of training and specific features.

495 If nothing else, these considerations indicate the urgent need for developing a more
496 nuanced conceptual approach and terminology to capture the intricacies of different types
497 of ‘meaning’, and a more appropriate language to talk about the relationship between
498 ‘features’ and ‘meaning’. Without a clearer theoretical framework, it will be difficult to
499 experimentally settle debates regarding the role of ‘meaning’ in natural scene perception.

500 In any case, the insensitivity to semantic inconsistencies reveals inherent limitations of both
501 MMs and DGII. The way in which MMs are constructed implicitly assumes that meaning is a
502 local image-property, which is not true for object-context (in)consistency. This limitation
503 may potentially be alleviated by ‘contextualized MMs’ (Peacock, Hayes, & Henderson,
504 2019), a recently suggested modification of the ‘standard’ MMs. These novel maps are
505 created from meaningfulness ratings by observers who see the whole scenes from which
506 the to-be-rated patches were derived. It is yet to be seen what this approach can reveal
507 about fixation selection beyond the fact that humans asked to indicate meaningful or
508 interesting regions within scenes highlight areas, which tend to be frequently fixated by
509 other observers (Nyström & Holmqvist, 2008; Onat et al., 2014). DGII, in turn, does not

510 explicitly encode semantic information, and was not trained on the relationship between
511 eye movements and semantic (in)consistency. But its failure highlights an opportunity to
512 improve saliency models by incorporating semantic relationships (Bayat, Koh, Nand, Pereira,
513 & Pomplun, 2018).

514 Taken together, our results suggest that, contrary to their core promise as a methodology,
515 meaning maps (MMs) do not offer a way to measure the spatial distribution of meaning
516 across an image. Instead of meaning per-se, they seem to index high-level features that
517 have the potential to carry meaning in typical natural scenes. They share this characteristic
518 with state-of-the-art saliency models, which are easier to use, do not require human
519 annotation, and yet predict locations of human fixations better than MMs.

520

521

References

522 Bayat, A., Koh, D. H., Nand, A. K., Pereira, M., & Pomplun, M. (2018). Scene Grammar in
523 Human and Machine Recognition of Objects and Scenes. In *Proceedings of the IEEE*
524 *Conference on Computer Vision and Pattern Recognition Workshops*.
525 <https://doi.org/10.1109/CVPRW.2018.00268>

526 Borji, A., Sihite, D. N., & Itti, L. (2013). Objects do not predict fixations better than early
527 saliency : A re-analysis of Einhauser et al.'s data. *Journal of Vision*, 13(2013), 1–4.
528 <https://doi.org/10.1167/13.10.18>

529 Bylinskii, Z., Judd, T., Borji, A., Itti, L., Durand, F., Oliva, A., & Torralba, A. (2014). MIT Saliency
530 Benchmark Results. Retrieved from <http://saliency.mit.edu/>

531 Bylinskii, Z., Judd, T., Oliva, A., Torralba, A., & Durand, F. (2016). What do different
532 evaluation metrics tell us about saliency models? *ArXiv*. Retrieved from
533 <http://arxiv.org/abs/1604.03605>

534 Elazary, L., & Itti, L. (2008). Interesting objects are visually salient. *Journal of Vision*, 8(3), 1–
535 15. <https://doi.org/10.1167/8.3.3>

536 Garcia-Diaz, A., Fdez-Vidal, X. R., Pardo, X. M., & Dosil, R. (2012). Saliency from hierarchical
537 adaptation through decorrelation and variance normalization. *Image and Vision*

- 538 *Computing*, 30(1), 51–64. <https://doi.org/10.1016/j.imavis.2011.11.007>
- 539 Harel, J., Koch, C., & Perona, P. (2006). Graph-Based Visual Saliency. *Advances in Neural*
540 *Information Processing Systems 19*, 19, 545–552. <https://doi.org/10.1.1.70.2254>
- 541 Hayes, T. R., & Henderson, J. M. (2019). Center bias outperforms image salience but not
542 semantics in accounting for attention during scene viewing. *Attention, Perception, &*
543 *Psychophysics*. <https://doi.org/https://doi.org/10.3758/s13414-019-01849-7>
- 544 Hayhoe, M., & Ballard, D. (2005). Eye movements in natural behavior. *Trends in Cognitive*
545 *Sciences*, 9(4). <https://doi.org/10.1016/j.tics.2005.02.009>
- 546 Hegde, J., & Kersten, D. (2010). A Link between Visual Disambiguation and Visual Memory.
547 *Journal of Neuroscience*, 30(45), 15124–15133.
548 <https://doi.org/10.1523/JNEUROSCI.4415-09.2010>
- 549 Henderson, J. M. (2017). Gaze Control as Prediction. *Trends in Cognitive Sciences*, 21(1), 15–
550 23. <https://doi.org/10.1016/j.tics.2016.11.003>
- 551 Henderson, J. M., & Hayes, T. R. (2017). Meaning-based guidance of attention in scenes as
552 revealed by meaning maps. *Nature Human Behaviour*, 1(October).
553 <https://doi.org/10.1038/s41562-017-0208-0>
- 554 Henderson, J. M., & Hayes, T. R. (2018). Meaning guides attention in real-world scene
555 images: Evidence from eye movements and meaning maps. *Journal of Vision*, 18(6), 10.
556 <https://doi.org/10.1167/18.6.10>
- 557 Henderson, J. M., Hayes, T. R., Peacock, C. E., & Rehrig, G. (2019). Meaning and Attentional
558 Guidance in Scenes : A Review of the Meaning Map Approach. *Vision*, 3(2).
- 559 Henderson, J. M., Hayes, T. R., Rehrig, G., & Ferreira, F. (2018). Meaning Guides Attention
560 during Real-World Scene Description. *Scientific Reports*, 8(1), 13504.
561 <https://doi.org/10.1038/s41598-018-31894-5>
- 562 Henderson, J. M., Malcolm, G. L., & Schandl, C. (2009). Searching in the dark: Cognitive
563 relevance drives attention in real-world scenes. *Psychonomic Bulletin & Review*, 16(5),
564 850–856. <https://doi.org/10.3758/PBR.16.5.850>
- 565 Henderson, J. M., Weeks, P. A., & Hollingworth, A. (1999). The effects of semantic

- 566 consistency on eye movements during complex scene viewing. *Journal of Experimental*
567 *Psychology: Human Perception and Performance*, 25(1), 210–228.
568 <https://doi.org/10.1037/0096-1523.25.1.210>
- 569 Itti, L., & Koch, C. (2000). A saliency-based search mechanism for overt and covert shifts of
570 visual attention. *Vision Research*, 40(10–12), 1489–1506.
571 [https://doi.org/10.1016/S0042-6989\(99\)00163-7](https://doi.org/10.1016/S0042-6989(99)00163-7)
- 572 Itti, L., & Koch, C. (2001). Computational modelling of visual attention. *Nature Reviews*
573 *Neuroscience*, 2(3), 194–203. <https://doi.org/10.1038/35058500>
- 574 Kaiser, D., Quek, G. L., Cichy, R. M., & Peelen, M. V. (2019). Object Vision in a Structured
575 World. *Trends in Cognitive Sciences*, 23(8), 672–685.
576 <https://doi.org/10.1016/j.tics.2019.04.013>
- 577 Kietzmann, T. C., McClure, P., & Kriegeskorte, N. (2019). Deep Neural Networks in
578 Computational Neuroscience. In *Oxford Research Encyclopedia of Neuroscience*.
- 579 Kleiner, M., Brainard, D., & Pelli, D. G. (2007). What's new in psychtoolbox-3? *Perception*,
580 36(1).
- 581 Koehler, K., Guo, F., Zhang, S., & Eckstein, M. P. (2014). What do saliency models predict?
582 *Journal of Vision*, 14(3). <https://doi.org/10.1167/14.3.14>
- 583 Kümmerer, M., Wallis, T. S. A., & Bethge, M. (2015). Information-theoretic model
584 comparison unifies saliency metrics. *Proceedings of the National Academy of Sciences*,
585 112(52), 16054–16059. <https://doi.org/10.1073/pnas.1510393112>
- 586 Kümmerer, M., Wallis, T. S. A., & Bethge, M. (2016). DeepGaze II: Reading fixations from
587 deep features trained on object recognition, 1–16. Retrieved from
588 <http://arxiv.org/abs/1610.01563>
- 589 Kümmerer, M., Wallis, T. S. A., & Bethge, M. (2018). Saliency Benchmarking Made Easy:
590 Separating Models, Maps and Metrics. In V. Ferrari, M. Hebert, C. Sminchisescu, & Y.
591 Weiss (Eds.), *Computer Vision – ECCV 2018. ECCV 2018. Lecture Notes in Computer*
592 *Science* (Vol. 11220, pp. 798–814). Springer. [https://doi.org/10.1007/978-3-030-01270-](https://doi.org/10.1007/978-3-030-01270-0_47)
593 [0_47](https://doi.org/10.1007/978-3-030-01270-0_47)

- 594 Kümmerer, M., Wallis, T. S. A., Gatys, L. A., & Bethge, M. (2017). Understanding Low- and
595 High-Level Contributions to Fixation Prediction. In *The IEEE International Conference on*
596 *Computer Vision (ICCV)*. <https://doi.org/10.1109/ICCV.2017.513>
- 597 Malcolm, G. L., Groen, I. I. A., & Baker, C. I. (2016). Making Sense of Real-World Scenes.
598 *Trends in Cognitive Sciences*, 20(11), 843–856.
599 <https://doi.org/10.1016/j.tics.2016.09.003>
- 600 Nyström, M., & Holmqvist, K. (2008). Semantic override of low-level features in image
601 viewing—both initially and overall. *Journal of Eye Movement Research*, 2(2), 1–11.
602 <https://doi.org/10.16910/jemr.2.2.2>
- 603 Öhlschläger, S., & Vö, M. L. H. (2017). SCEGRAM: An image database for semantic and
604 syntactic inconsistencies in scenes. *Behavior Research Methods*, 49(5).
605 <https://doi.org/10.3758/s13428-016-0820-3>
- 606 Onat, S., Açıık, A., Schumann, F., & König, P. (2014). The contributions of image content and
607 behavioral relevancy to overt attention. *PLoS ONE*, 9(4).
608 <https://doi.org/10.1371/journal.pone.0093254>
- 609 Parkhurst, D., Law, K., & Niebur, E. (2002). Modeling the role of salience in the allocation of
610 overt visual attention. *Vision Research*, 42(1), 107–123. [https://doi.org/10.1016/S0042-](https://doi.org/10.1016/S0042-6989(01)00250-4)
611 [6989\(01\)00250-4](https://doi.org/10.1016/S0042-6989(01)00250-4)
- 612 Peacock, C. E., Hayes, T. R., & Henderson, J. M. (2018). Meaning guides attention during
613 scene viewing, even when it is irrelevant. *Attention, Perception, and Psychophysics*, 20–
614 34. <https://doi.org/10.3758/s13414-018-1607-7>
- 615 Peacock, C. E., Hayes, T. R., & Henderson, J. M. (2019). The role of meaning in attentional
616 guidance during free viewing of real-world scenes. *Acta Psychologica*, 198(June).
617 <https://doi.org/10.1016/j.actpsy.2019.102889>
- 618 Rider, A. T., Coutrot, A., Pellicano, E., Dakin, S. C., & Mareschal, I. (2018). Semantic content
619 outweighs low-level saliency in determining children’s and adults’ fixation of movies.
620 *Journal of Experimental Child Psychology*, 166, 293–309.
621 <https://doi.org/10.1016/j.jecp.2017.09.002>

- 622 Rouder, J. N., Speckman, P. L., Sun, D., Morey, R. D., & Iverson, G. (2009). Bayesian t tests for
623 accepting and rejecting the null hypothesis. *Psychonomic Bulletin and Review*, *16*(2),
624 225–237. <https://doi.org/10.3758/PBR.16.2.225>
- 625 Simonyan, K., & Zisserman, A. (2014). Very Deep Convolutional Networks for Large-Scale
626 Image Recognition. *CoRR, Abs/1409.1556*. Retrieved from
627 <http://arxiv.org/abs/1409.1556>
- 628 Stoll, J., Thrun, M., Nuthmann, A., & Einhäuser, W. (2015). Overt attention in natural scenes:
629 Objects dominate features. *Vision Research*, *107*, 36–48.
630 <https://doi.org/10.1016/j.visres.2014.11.006>
- 631 Tatler, B. (2007). The central fixation bias in scene viewing: Selecting an optimal viewing
632 position independently of motor biases and image feature distributions. *Journal of*
633 *Vision*, *7*(4), 1–17. <https://doi.org/10.1167/7.14.4>
- 634 Tatler, B. W., Hayhoe, M. M., Land, M. F., & Ballard, D. H. (2011). Eye guidance in natural
635 vision: Reinterpreting salience. *Journal of Vision*, *11*(5), 5–5.
636 <https://doi.org/10.1167/11.5.5>
- 637 Teufel, C., Dakin, S. C., & Fletcher, P. C. (2018). Prior object-knowledge sharpens properties
638 of early visual feature- detectors. *Scientific Reports*, (June), 1–12.
639 <https://doi.org/10.1038/s41598-018-28845-5>
- 640 Võ, M. L. H., Boettcher, S. E., & Draschkow, D. (2019). Reading scenes: how scene grammar
641 guides attention and aids perception in real-world environments. *Current Opinion in*
642 *Psychology*, *29*, 205–210. <https://doi.org/10.1016/j.copsyc.2019.03.009>
- 643 Wilming, N., Onat, S., Ossandón, J. P., Açik, A., Kietzmann, T. C., Kaspar, K., Gameiro, R. R.,
644 Vormberg, A., & König, P. (2017). An extensive dataset of eye movements during viewing of
645 complex images. *Scientific Data*, *4*, 1–11. <https://doi.org/10.1038/sdata.2016.126>
- 646 Zhang, L., Tong, M. H., Marks, T. K., & Cottrell, G. W. (2008). SUN: A Bayesian framework for
647 saliency using natural statistics. *Journal of Vision*, *8*(32). <https://doi.org/10.1167/8.7.32>